

# D-TRANSFORM BASED CONTROL OF POWER CONVERTERS

A. H. R. Rosa<sup>1</sup>, W. W. A. G. Silva<sup>2</sup>, W. He<sup>3</sup>, F. A. da Silva<sup>1</sup>, L. M. F. Morais<sup>4</sup>, S. I. Seleme Jr.<sup>4</sup>

<sup>1</sup>Instituto Federal de Minas Gerais (IFMG Campus Betim), Betim – MG, Brasil

<sup>2</sup>Universidade Federal de Itajubá (UNIFEI) – MG, Brasil

<sup>3</sup>School of Automation, Nanjing University of Information Science and Technology – China

<sup>4</sup>Universidade Federal de Minas Gerais (UFMG) – MG, Brasil

e-mail: arthurhrosa@gmail.com

**Abstract** – The aim of this study is to present a very simple, intuitive and feasible tool: the D-transform between converters. This new method proposes to find a control equation of any pre-defined control law from one converter to another power converter. The central goal is to take maximum advantage of the robustness offered by the originator nonlinear control law. Although there is the possibility of more than one conversion, some candidates show good performance in terms of transient overshoot, settling time and steady-state regulation. The stability proof is disposed individually for each generated equation. The performance of D-Controllers is verified through Hardware In the Loop (HIL) simulations. A small overshoot under input and load perturbations is achieved for the buck-boost example. Finally, a experimental validation using a buck converter is given to illustrate the application method and the nonlinear control design.

**Keywords** – Boost, Buck, Buck-Boost, D-Transform, HIL Simulation, IDAPBC, Nonlinear Control, Relations, SFL.

## NOMENCLATURE

$E$	Input voltage.
$\mu$	Generalized duty cycle.
$U$	Steady-State duty cycle.
$D$	Boost duty cycle.
$d$	Buck duty cycle.
$\delta$	Buck-boost duty cycle.
$x_1$	Inductor current.
$x_2$	Capacitor voltage.
$V_d$	Desired output voltage.
$x_{2d}$	Output voltage reference.
$L$	Converters inductance.
$C$	Converters capacitance.
$G$	Load conductance.
$R$	Load resistance.
$x'$	Complementer operator (1-x).
$\bar{x}$	Steady-state value.
$k_1$	SFL gain controller.
$k_\alpha$	CIDAPBC gain controller.
$k_z$	IDAPBC gain controller.

## I. INTRODUCTION

The design of non-conventional methods for solving power electronics and control problems is an emerging area [1], [2]. There are many reasons to use non-classical techniques, such as energy savings, cost reductions and, obviously, the increase of dynamic performance, large stability margin, and high robustness [3], [4], [5]. Therefore, this paper presents a new perspective regarding the control of static power converters that play a key role in several emerging applications including power systems [6], transformers [7], dc micro-grids [8] - [9], electric vehicles and aircrafts [10] - [11], integrated energy systems [12], photovoltaic systems [13] 1, cyber-physical systems [2], inverters [14], etc. . .

Through the employment of average nonlinear dynamic model, different nonlinear control methods have been addressed to regulate the desired voltage or current and achieve the stability of the closed-loop system [15]. Nonlinear controllers have been successfully applied to dc/dc converters established by a rigorous mathematical formulation, and are, in many cases, combined with the traditional PI control [16]. Nevertheless, almost all of the existing control methods for dc/dc converters requisite exact knowledge of the converter parameters (capacitance, inductance) or the load impedance to assurance nonlinear stability.

The Laplace, Fourier and Z-transforms [17] are remarkable tools in different domains, e.g., control, signal processing, telecommunications and electronic engineering. The central purpose is to directly apply the preferred and simplified equations that can be used in several practical applications. Inspired by this motion, we aim at designing a transform function of converter equations. To be specific, this work outlines a methodology to achieve nonlinear control based on D-Transform, which will be better described in dedicated section.

The first reason is the rapid generation of control equations extended of one converter to another. The second motivation is to produce a new family of controllers based on previously developed equations that will be redesigned. Such new control laws meet the requirements for new insights and robustness criteria of advanced controllers.

What is the D-Transform? By definition, the D-transform is comprised of finding, straightly, a function that converts an equation of the duty cycle  $\mu$  from one converter to another converter, through the existing input to output relations of these converters, which are functions of the duty-cycle.

Moreover, the control methods used in this work are the State Feedback Linearization (SFL) [18] – [19], Interconnection and Damping Assignment Passivity-Based

---

Manuscript received 11/09/2021; first revision 12/14/2021; accepted for publication 04/16/2022, by recommendation of Editor Marcelo Lobo Heldwein. <http://dx.doi.org/10.18618/REP.2022.1.0046>

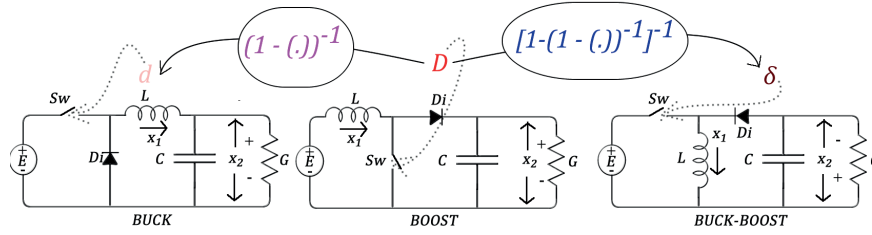


Fig. 1. Typical power converters and proposed D-Transform. Buck duty cycle ( $d$ ), Boost duty cycle ( $D$ ), and Buck-boost duty cycle ( $\delta$ ).

**TABLE I**  
**Converters Models**

	Boost	Buck	Buck-Boost
SSM	$\dot{x}_1 = -(1-\mu)\frac{1}{L}x_2 + \frac{E}{L}$ $\dot{x}_2 = (1-\mu)\frac{1}{C}x_1 - \frac{G}{C}x_2$	$\dot{x}_1 = -\frac{1}{L}x_2 + \mu\frac{E}{L}$ $\dot{x}_2 = \frac{1}{C}x_1 - \frac{G}{C}x_2$	$\dot{x}_1 = (1-\mu)\frac{1}{L}x_2 + \mu\frac{E}{L}$ $\dot{x}_2 = -(1-\mu)\frac{1}{C}x_1 - \frac{G}{C}x_2$
SSM <sub>n</sub> <sup>0*</sup>	$\dot{x}_{1n} = -\mu'x_{2n} + 1$ $\dot{x}_{2n} = \mu x_{1n} - \frac{1}{Q}x_{2n}$	$\dot{x}_{1n} = -x_{2n} + \mu$ $\dot{x}_{2n} = x_{1n} - \frac{1}{Q}x_{2n}$	$\dot{x}_{1n} = \mu'x_{2n} + \mu$ $\dot{x}_{2n} = -\mu'x_{1n} - \frac{1}{Q}x_{2n}$
ELM	$D_B\dot{x} + (1-\mu)J_Bx + R_Bx = F$ $J_B = \begin{bmatrix} 0 & 1 \\ -1 & 0 \end{bmatrix};$ $x = \begin{bmatrix} x_1 \\ x_2 \end{bmatrix}; D_B = \begin{bmatrix} L & 0 \\ 0 & C \end{bmatrix}; R_B = \begin{bmatrix} 0 & 0 \\ 0 & G \end{bmatrix}; F = \begin{bmatrix} E \\ 0 \end{bmatrix}$	$D_B\dot{x} + (J_B + R_B)x = \mu F$ $J_B = \begin{bmatrix} 0 & 1 \\ -1 & 0 \end{bmatrix}$	$D_B\dot{x} + (1-\mu)J_Bx + R_Bx = \mu F$ $J_B = \begin{bmatrix} 0 & -1 \\ 1 & 0 \end{bmatrix};$
PHC	$J_H = \begin{bmatrix} 0 & -\frac{1-\mu}{LC} \\ \frac{1-\mu}{LC} & 0 \end{bmatrix};$ $R_H = \begin{bmatrix} 0 & 0 \\ 0 & \frac{1}{RC^2} \end{bmatrix}; g_H = \begin{bmatrix} \frac{1}{L} \\ 0 \end{bmatrix}$ $x = \begin{bmatrix} x_1 \\ x_2 \end{bmatrix}; \dot{x} = [J_H(\mu) - R_H] \frac{\partial H}{\partial x}(x) + g_H E; H(x) = \frac{1}{2}Lx_1^2 + \frac{1}{2}Cx_2^2$	$J_H = \begin{bmatrix} 0 & -\frac{1}{LC} \\ \frac{1}{LC} & 0 \end{bmatrix};$ $R_H = \begin{bmatrix} 0 & 0 \\ 0 & \frac{1}{RC^2} \end{bmatrix}; g_H = \begin{bmatrix} \frac{\mu}{L} \\ 0 \end{bmatrix};$	$J_H = \begin{bmatrix} 0 & \frac{1-\mu}{LC} \\ -\frac{1-\mu}{LC} & 0 \end{bmatrix};$ $R_H = \begin{bmatrix} 0 & 0 \\ 0 & -\frac{1}{RC^2} \end{bmatrix}; g_H = \begin{bmatrix} \frac{\mu}{L} \\ 0 \end{bmatrix};$

Control (IDA-PBC) [20] and other nonlinear control equations derived via D-Transform, whose models and control formulations are demonstrated in section II. The proposed D-Transform approach is explained in section III. Finally, results and conclusions are presented in section IV and V.

## II. MODELING AND RELATIONS BETWEEN CONVERTERS

The basic dc-dc power converters - as boost, buck, and buck-boost shown in Figure 1 - are typical building blocks in power electronics, that have the same elements: one diode, one switch, one capacitor and one inductor. The difference between them comprises the physical position of such elements. Furthermore, the nonlinear behaviour is mainly present on semiconductor components (diode and switch).

Table I condenses three distinct models commonly found in the literature: Euler-Lagrange Model (ELM), State-Space Model (SSM) and Port-Controlled Hamiltonian (PCH). It should be emphasized that the Euler-Lagrange approach presents an equivalent form of buck-boost and boost modelling. In sequence, PCH model evidences a similar structure for the three converters. Possible problems encountered in boost and buck-boost converters are related to the occurrence of right-half-plane (RHP) zeros, which troublesome characteristic brings to nonminimum-phase [21]. Additionally, RHP zero is the origin of bandwidth limitation and instability of closed-loop system [22].

*normalized models are obtained by considering [23]:*  $\tau = \frac{1}{\sqrt{LC}}, x_{1n} = \frac{1}{E}\sqrt{\frac{L}{C}}x_1, x_{2n} = \frac{1}{E}x_2, \dot{x}_{in} = \frac{x_{in}}{\tau}$

### A. Equilibrium's Relation of Power Converters

The relations addressed in the following sentences - and summarized in Table II - are reported by the majority of power electronics book. Even so, we replicate some essential relations that will be employed to attain the proposed D-transform. It can be noted that these relations are for the ideal DC-DC converters in CCM (Continuous Current Mode) operation.

#### Boost

The circuit of boost converter circuit can be modelled by average space state equations:

$$\dot{x}_1 = -(1-D)\frac{1}{L}x_2 + \frac{E}{L}; \dot{x}_2 = (1-D)\frac{1}{C}x_1 - \frac{G}{C}x_2. \quad (1)$$

where  $x_1$  denotes the inductor current,  $x_2$  is the capacitor voltage,  $E$  is the input voltage,  $x_n$  is the normalized state variable.

In the steady state, by substituting  $\dot{x}_1 = 0$  and  $\dot{x}_2 = 0$  in (1), the equilibrium points of the boost converter are given by:

$$\bar{x}_1 = \frac{EG}{(1-D)^2}, \bar{x}_2 = \frac{E}{(1-D)}. \quad (2)$$

By considering  $\bar{D}$  as a constant control input in view of (2), one gets:

$$\bar{x}_1 = \frac{G}{E}\bar{x}_2^2. \quad (3)$$

Now, replacing the desired output capacitor voltage as  $\bar{x}_2 = V_d$ , the equilibrium points  $\bar{x}$  and the fixed input control

**TABLE II**  
**Relation Equations**

	SFL control equation	Open loop ( $U = \bar{d}, \bar{D}, \bar{\delta}$ )		Slew rate	$\frac{V_d}{E}$	Transformation
Buck	$d = \frac{-k_1(x_1 - x_{1d}) + x_2}{E}$	$\bar{d} = 1 - \frac{E - V_d}{E}$	$\bar{d} = \frac{V_d}{E}$	$\bar{d}' = 1 - \bar{d} = \frac{E - V_d}{E}$	$\mu$	$d = (D')^{-1}$
Boost	$D = 1 - \frac{[E + k_1(x_1 - x_{1d})]}{x_2}$	$\bar{D} = 1 - \frac{E}{V_d}$	$\bar{D} = \frac{V_d - E}{V_d}$	$\bar{D}' = 1 - \bar{D} = \frac{E}{V_d}$	$\frac{1}{(1-\mu)}$	$\frac{1}{(1-D)}$
Buck-Boost	$\delta = \frac{+k_1(x_1 - x_{1d}) + x_2}{x_2 - E}$	$\bar{\delta} = 1 - \frac{E}{E - V_d}$	$\bar{\delta} = \frac{V_d}{E - V_d}$	$\bar{\delta}' = 1 - \bar{\delta} = \frac{E}{E - V_d}$	$-\frac{\mu}{(1-\mu)}$	$-\frac{\delta}{(1-\delta)}$

**TABLE III**  
**Transfer Functions (Found in [24])**

Converter	$G_{i0}$	$G_{d0}$	$w_0$	$Q$	$w_z$
Buck	$U$	$\frac{V_d}{U}$	$\frac{1}{\sqrt{LC}}$	$R\sqrt{\frac{C}{L}}$	$\infty$
Boost	$\frac{1}{U'}$	$\frac{V_d}{U'}$	$\frac{U'}{\sqrt{LC}}$	$U'R\sqrt{\frac{C}{L}}$	$\frac{U'2R}{L}$
Buck-boost	$\frac{-U}{U'}$	$\frac{V_d}{U'}$	$\frac{U'}{\sqrt{LC}}$	$U'R\sqrt{\frac{C}{L}}$	$\frac{U'2R}{UL}$

$\bar{D}$  are given by:

$$\bar{D} = 1 - \frac{E}{V_d}, \bar{x} = [\bar{x}_1, \bar{x}_2]^T = \left[ GV_d \left( \frac{V_d}{E} \right), V_d \right]^T. \quad (4)$$

*Buck*

Next let us consider the buck converter, some simple calculations show that:

$$\bar{x}_1 = dEG, \bar{x}_2 = dE, \bar{x}_1 = G\bar{x}_2, \bar{d} = 1 - \frac{E - V_d}{E}, \quad (5)$$

$$\bar{x} = [\bar{x}_1, \bar{x}_2]^T = [GV_d, V_d]^T.$$

The State-Space Modelling of step down converter is given by:

$$\dot{x}_1 = -\frac{1}{L}x_2 + d\frac{E}{L}, \quad (6)$$

$$\dot{x}_2 = \frac{1}{C}x_1 - \frac{G}{C}x_2, \quad (7)$$

The equilibrium points of buck converter is obtained when replacing  $\dot{x} = 0$  in (6)-(7):

$$\bar{x}_1 = dEG, \quad (8)$$

$$\bar{x}_2 = dE. \quad (9)$$

By considering  $d$  as a fixed value in (8)-(9) leads to:

$$\bar{x}_1 = G\bar{x}_2. \quad (10)$$

Therefore, the fixed open loop control  $\bar{d}$  to stabilize  $\bar{x}$  is:

$$\bar{d} = 1 - \frac{E - V_d}{E}, \quad (11)$$

$$\bar{x} = [\bar{x}_1, \bar{x}_2]^T = [GV_d, V_d]^T.$$

*Buck-boost*

The equivalent SSM of buck-boost can be expressed in the following form:

$$\dot{x}_1 = (1 - \delta)\frac{1}{L}x_2 + \delta\frac{E}{L}, \quad (12)$$

$$\dot{x}_2 = -(1 - \delta)\frac{1}{C}x_1 - \frac{G}{C}x_2, \quad (13)$$

When substituting  $\dot{x}_1 = 0$  and  $\dot{x}_2 = 0$  in (12)-(13), one obtains:

$$\bar{x}_1 = \frac{\delta EG}{(1 - \delta)^2}. \quad (14)$$

$$\bar{x}_2 = -\frac{\delta E}{(1 - \delta)}. \quad (15)$$

By replacing  $\bar{\delta}$  in (14)-(15), we have:

$$\bar{x}_1 = G\bar{x}_2 \left( \frac{\bar{x}_2}{E} - 1 \right). \quad (16)$$

Thus, the equilibrium points to stabilize  $\bar{x}$  and the constant input control  $\bar{\delta}$  given by:

$$\bar{\delta} = 1 - \frac{E}{E - V_d}, \quad (17)$$

$$\bar{x} = [\bar{x}_1, \bar{x}_2]^T = \left[ GV_d \left( \frac{V_d}{E} - 1 \right), V_d \right]^T.$$

So, the summarized equations for buck-boost converter are:

$$\bar{x}_1 = \frac{\delta EG}{(1 - \delta)^2}, \bar{x}_2 = -\frac{\delta E}{(1 - \delta)}, \bar{x}_1 = G\bar{x}_2 \left( \frac{\bar{x}_2}{E} - 1 \right),$$

$$\bar{\delta} = 1 - \frac{E}{E - V_d}, \bar{x} = [\bar{x}_1, \bar{x}_2]^T = \left[ GV_d \left( \frac{V_d}{E} - 1 \right), V_d \right]^T. \quad (18)$$

### B. Transfer Functions of Linearized Models

Table III exhibits parameters of both control-to-output ( $G_{vd}$ ) and input-to-output ( $G_{vi}$ ) transfer functions of the basic boost, buck and buck-boost converters [24]:

$$G_{vi}(s) = G_{i0} \frac{1}{1 + \frac{s}{Qw_0} + \left(\frac{s}{w_0}\right)^2}, \quad (19)$$

**TABLE IV**  
**Canonical Circuit Parameter (Found in [24])**

Converter	$M(U)$	$L_e$	$e(s)$	$j(s)$
Buck	$U$	$L$	$\frac{V_d}{U^2}$	$\frac{V_d}{R}$
Boost	$\frac{1}{U'}$	$\frac{L}{U'^2}$	$V_d \left(1 - \frac{sL}{U'^2 R}\right)$	$\frac{V_d}{U'^2 R}$
Buck-boost	$\frac{-U}{U'}$	$\frac{L}{U'^2}$	$\frac{-V_d}{U'^2} \left(1 - \frac{sL}{U'^2 R}\right)$	$\frac{-V_d}{U'^2 R}$

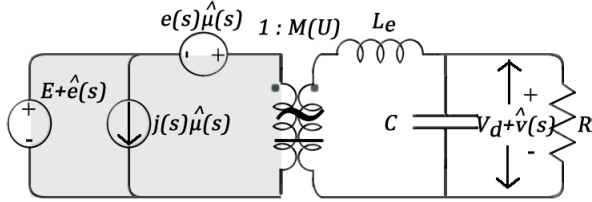


Fig. 2. Canonical power converters circuits.

$$G_{vd}(s) = G_{d0} \frac{\left(1 - \frac{s}{w_z}\right)}{\left(1 + \frac{s}{Qw_0} + \left(\frac{s}{w_0}\right)^2\right)}. \quad (20)$$

The canonical form of converters is shown in Figure 2. The straight derivation of the transfer functions is displayed in Table IV. All tables presented in this work make an effort to clarify common characteristics among the converts, so they are customized as potential sources of D-candidates.

### III. MAIN IDEA: THE D-TRANSFORM

Figure 3 shows the flowchart of the proposed methodology. The D-Transform design proceeds in following steps:

1. Converter: choose a converter as a starting point. In this work, the boost was selected.
2. Inputs: it is possible to apply any nonlinear control based equations. We use SFL and IDAPBC control laws, for example.
3. D-Transform: the next step is to apply the D-transform, firstly, by considering intuitive relations (e.g.: steady-state equations), and then nontrivial relations.
4. Outputs: the new D-Controllers (e.g.: D-SFL, D-CIDAPBC, D-IDAPBC).
5. Validation: finally, the new generated control equations can be verified by software simulations, stability analysis and hardware tests.

**Definition 1.** The D-transform consists of finding, directly, a function that establishes the duty cycle  $\mu$  from one converter to another.

Surrounded by several candidates, we choose as initial point the following transformation equations:

**Proposition 1.** There is a transformation function  $\Delta_1$  that converts  $D \rightarrow d, \delta$ :

$$d, \delta = \Delta_1(D), d = (D')^{-1}, \delta = 1 - [1 - (D')^{-1}]^{-1}. \quad (21)$$

**Example 1.** The root of  $\Delta_1$  is related to steady-state investigation. To simplify the notation, let us replicate the buck and boost equations given by (4)-(5):

$$\bar{D} = \frac{V_d - E}{V_d}, \bar{d} = \frac{V_d}{E}. \quad (22)$$

It is possible to define an expression that leads  $\bar{D} \Rightarrow \bar{d}$  (consequently,  $D \Rightarrow d$ ). It should be noted that the equation conversion is given by (21) and the second column of Table III.

**Proposition 2.** There exist other transformation functions  $\Delta_2, \Delta_3, \dots, \Delta_n$  that convert  $D \rightarrow \delta$ :

$$\delta = \Delta_2(D), \delta = -\frac{D^{-1}}{D'} \quad (23)$$

$$\delta = \Delta_3(D), \delta = 1 + D'. \quad (24)$$

**Example 2.** Let us repeat the control gain  $G_{io}$  of Table III:

$$G_{io} = \frac{-U}{U'}, \quad (25)$$

By replacing  $U$  - generalized duty cycle in steady-state - by  $D$  it is important to recall that (23) and (25) are similar.

To investigate the applications of D-transform we choose recently nonlinear equations found in the literature. For simplicity, we use two control laws based on IDAPBC. In [25], Classic IDAPBC (referenced as CIDAPBC) is addressed to boost converters achieving a simple control equation described by: CIDAPBC:

$$\bar{D} = 1 - \frac{E}{V_d}, D = 1 - (1 - \bar{D}) \left(\frac{x_2}{V_d}\right)^{k_\alpha}. \quad (26)$$

In addition, [20] modify and improve (26) to obtain: IDAPBC:

$$D = 1 - \frac{k_z E}{2E x_2 + (k_z - 2E) x_{2d}}. \quad (27)$$

For didactic purposes, we also add the nonlinear SFL equation [15]:

$$D = 1 - \frac{[E + k_1(x_1 - x_{1d})]}{x_2}. \quad (28)$$

By replacing the results of (26)-(28) in (21)-(24), we collect the new D-equations gathered in Table II (where  $k_1, k_\alpha$  and  $k_z$  are the nonlinear control gains).

**Example 3.** So, the new D-SFL control equation is performed by evaluation of (21) and (28):

$$d = \frac{x_2}{[E + k_1(x_1 - x_{1d})]}. \quad (29)$$

**Example 4.** By substituting (27) in (24):

$$\delta = 1 + \frac{k_z E}{2E x_2 + (k_z - 2E) x_{2d}}. \quad (30)$$

#### A. Stability Analyses

Two main goals are to be analyzed, regarding the stability of the closed-loop system: (i) the equilibrium of the system and (ii) the zero dynamics at the equilibrium. The control design consists in, first, rendering the error  $(x - x_d)$  equal to zero, and, there, ensuring asymptotic stability to the error dynamics.

**TABLE V**  
**D-Transform Control Equations**

	SFL	D-SFL	IDAPBC	D-IDAPBC
Buck	$d = \frac{-k_1(x_1 - x_{1d}) + x_2}{E}$	$d = \frac{x_2}{E + k_1(x_1 - x_{1d})}$	← Eq.(21) →	$d = \frac{2Ex_2 + (k-2E)x_2d}{kE}$
Boost (source)	$D = 1 - \frac{E + k_1(x_1 - x_{1d})}{x_2}$	-	$D' = \frac{kE}{2Ex_2 + (k-2E)x_2d}$	-
Buck-Boost	$\delta = \frac{+k_1(x_1 - x_{1d}) + x_2}{x_2 - E}$	$\delta = \frac{-x_2}{k_1(x_1 - x_{1d}) + E - x_2}$	← Eq.(21) Eq.(24) → → → → →	$\delta = 1 + \frac{kE}{2Ex_2 + (k-2E)x_2d}$

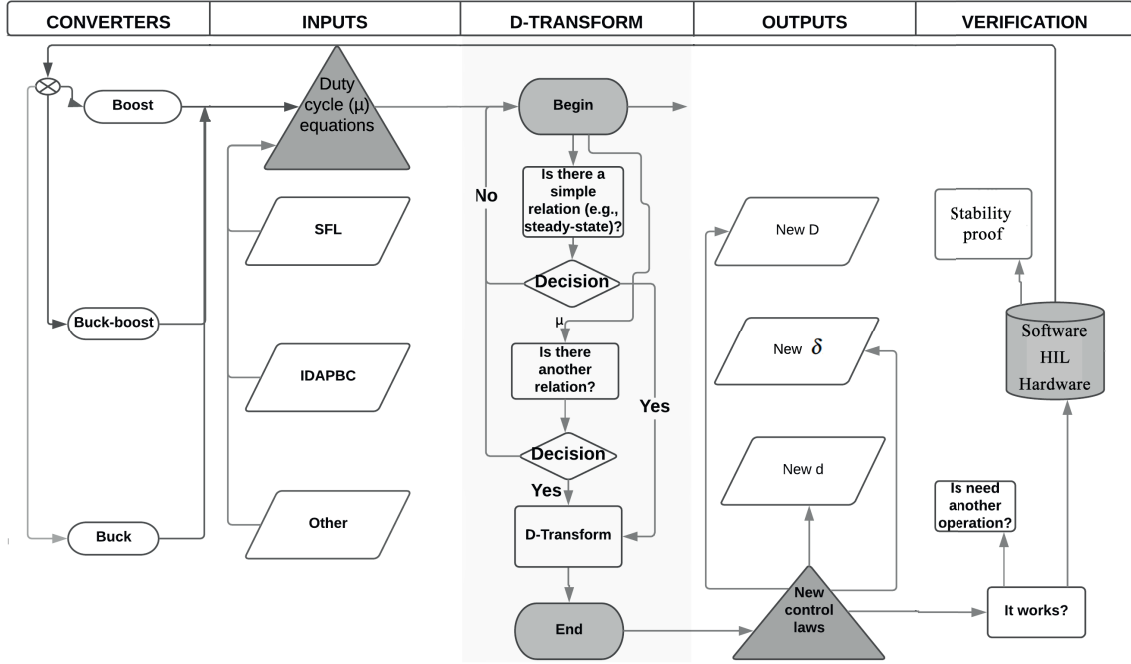


Fig. 3. Flowchart of D-Transform.

**TABLE VI**  
**D-Transform Control Equations**

	CIDAPBC	D-CIDAPBC
Buck	-	$d = 1 - (1 - \bar{d}) \left( \frac{x_2}{\bar{v}_d} \right)^{-k\alpha}$
Boost	$D = 1 - (1 - \bar{D}) \left( \frac{x_2}{\bar{v}_d} \right)^{k\alpha}$	-
Buck-Boost	-	$\delta = 1 - (1 - \bar{\delta}) \left( \frac{x_2}{\bar{v}_d} \right)^{k\alpha}$

As proved by [26], the system is asymptotically stable if the new control law is satisfied and the ‘zero dynamics’ around the desired equilibrium point are stable. In order to evaluate the stability of the internal dynamics of the closed loop system, the standard approach is to consider the corresponding zero dynamics. As long as the zero dynamics is asymptotically stable, the internal dynamics will be locally exponentially stable [27]. Thus, the equation describing the zero-order dynamics is obtained by making the error equal to zero and replacing the state variables by their respective steady-state values.

**Example 5.** The zero-order dynamics of the D-SFL buck control equation is obtained by using terms of (5) and (29):

$$\bar{\mu} = \frac{x_{20}}{E}, \quad (31)$$

$$\dot{x}_{20} = \frac{\bar{x}_1 - G\bar{x}_2}{C}. \quad (32)$$

As  $\bar{x}_2 = \bar{\mu}E$  and  $\bar{d} = \bar{\mu}$  for the buck converter, deriving the two sides of (31) and substituting in (32), the zero order dynamics as a function of  $\bar{\mu}$ :

$$\dot{\bar{\mu}} = \frac{G}{C} \left( \bar{\mu} - \frac{\bar{x}_1}{GE} \right) \quad (33)$$

which the equilibrium point,  $\bar{\mu} = \frac{\bar{x}_1}{GE}$ , is stable (similar procedure is obtained in [26] and [28]).

### B. D-Transform and $\delta$ -Transform

We choose the boost as base converter to generate D-Controllers for buck and buck-boost converters. However, the same strategy can be applied to attain the new D control laws from the buck (d-Transform) and also from the buck-boost ( $\delta$ -Transform). In other to clarify this suggestion, the evaluation of  $d \rightarrow \delta$  is given by:

$$\delta = 1 - (d')^{-1}. \quad (34)$$

The D-Controllers achieved for the buck-boost can be adapted to flyback converter, which is widely used in cellular power supplies and in other applications like LED and solar power

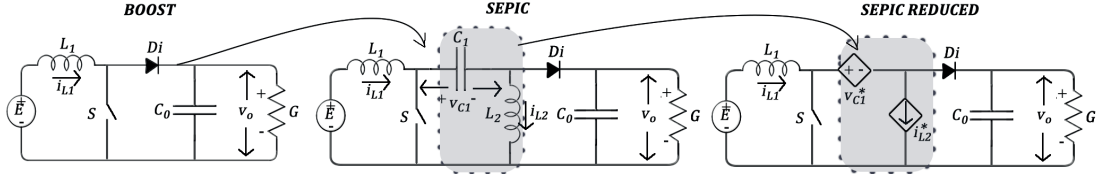


Fig. 4. Reduced SEPIC

system, for example [29]. For generation equations from buck to boost converter:

$$D = (d^{-1})'. \quad (35)$$

**Example 6.** Let us replicate the buck and boost equations given by (4)-(5):

$$\bar{D} = \frac{V_d - E}{V_d}, \bar{d} = \frac{V_d}{E}. \quad (36)$$

It is possible to define an expression that leads  $\bar{d} \Rightarrow \bar{D}$  (consequently,  $d \Rightarrow D$ ). It should be noted that the equation conversion is given by (35).

### C. Extension to Other Converters

Figure 4 shows the boost and SEPIC converters for comparison. It can be noted that when removing the intermediate elements ( $L_2, C_1$ ) highlighted by the dotted line, the SEPIC converter becomes similar to the boost converter, having similar equilibrium points as shown in Table VII.

Therefore, we can use the boost equations and apply them to control the SEPIC converter replacing the eliminated state variables ( $i_{L2}$  and  $v_{c1}$ ) by the equilibrium points, provided in Table VII, represented by dependent sources in the model. If we substitute, for example,  $v_{c1}$  by  $E$  and  $i_{L2}$  by  $GV_d$  in the SEPIC converter, it saves two sensors. Figure 4 summarizes this process. So the equation to transform the boost duty cycle  $D$  to SEPIC duty cycle  $D_s$  is:

$$D = D_s. \quad (37)$$

For CUK converter, Equation (37) can be applied as reported in [30].

### D. The Integral Action

The transformations, the nonlinear models and control equations require accurate knowledge of the converter parameters. Thus, in order to constrain the voltage output to get the desired value  $V_d$ , it is useful to include a proportional integrative (PI) term in the control equation, given by [31]:

$$G_{Int} = -k_{int} \int_0^t [x_2(s) - V_d] ds. \quad (38)$$

**TABLE VII**  
**Equilibrium Points of the Converters**

Converter	$i_{L1}^*$	$v_o^*$	$i_{L2}^*$	$v_{c1}^*$
Boost	$\frac{G}{E} V_d^2$	$V_d$	-	-
SEPIC	$\frac{G}{E} V_d^2$	$V_d$	$GV_d$	$E$

Equation (38) can be applied for all converters using D-Controllers, IDAPBC, SFL or other nonlinear control law. For example, by considering the D-SFL control and the buck converter:

$$d = \frac{x_{2d}}{[E + k_1(x_1 - x_{1d})]}, \quad (39)$$

$$x_{2d} = -k_{int} \int_0^t [x_2(s) - V_d] ds.$$

## IV. SOFTWARE SIMULATION AND HIL RESULTS

Simulations are made to compare the performance of D-Controllers using Matlab/Simulink and Single Hardware in The Loop (SHIL) approach [32]. In all simulations, we have chosen the system parameters and design specifications shown in Table 7 and the D-control laws (Tables V and VI).

In Figure 5.b we present the transient responses of the output voltage of the buck-boost under load perturbation, by considering original SFL and derived D-SFL, D-IDAPBC and D-CIDAPBC control methods. The same scheme is shown in Figure 5.c for the buck converter. In these simulations, consecutive load step variation of 70% to 100% are applied. Figure 5.a, D shows the output capacitor voltage  $x_2$  using Hardware in the loop. Figure 6 reveals the input variation tests.

As seen in Figures 4 and 5, both software simulations and HIL results reach the steady state value after the step variation. It is remarkable that the performance of the systems are in agreement, since the same transient dynamics is observed, even for the oscillatory dynamics. None of the implemented systems in software or in HIL presents instability. This attests that the embedded models and control equations are adequate to controlling the systems, and so, validating the control techniques. The processing time for the DSP (model Texas Instruments 28389D) to evaluate the control law and, consequently, to run a real-time simulation, is  $1.2 \mu s$ . Using a switching frequency  $f_s = 50 kHz$  ( $T_s = 20 \mu s$ ), the processing time of all control equations ( $< 1.5 \mu s$ ) demands 6% of the bandwidth.

## V. EXPERIMENTAL VALIDATION

The proposed control strategy was experimentally validated through a DC-DC converter prototype, Figure 12, development with kit BOOSTXL-3PHGANINV Evaluation Module of Texas Instruments [33]. The prototype consists of a three-phase GaN bridge module and a module of inductors and capacitors forming the passive elements of the buck and boost.

Figure 7 (PI) and Figure 8 (D-SFL) show the output voltage

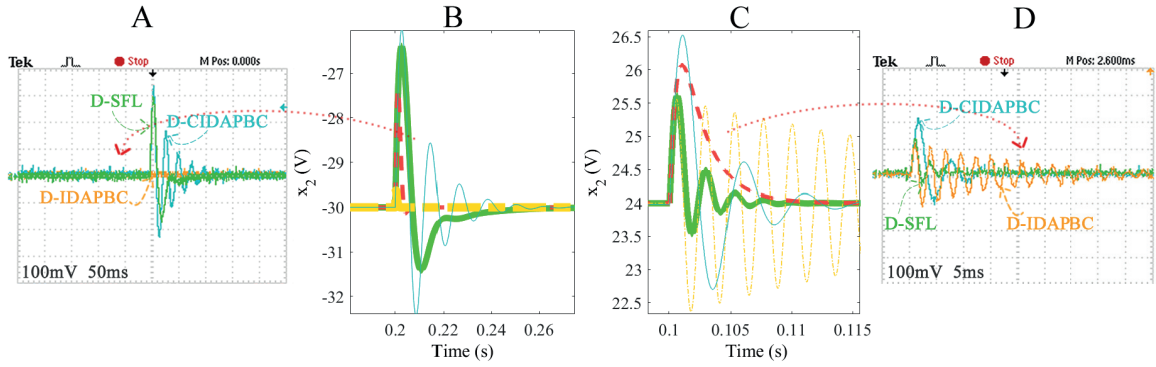


Fig. 5. Software simulation result (Matlab/Simulink) using control techniques SFL (dashed red), D-SFL (continue green) D-CICAPBC (continue cyan), D-IDAPBC (dashed yellow). Output voltage  $x_2$  for buck-boost (B) and buck (C) in view of load variation (70-100 %) in 0.1s and 0.2s. HIL experimental result, normalized output voltage  $x_2$  (A-D).

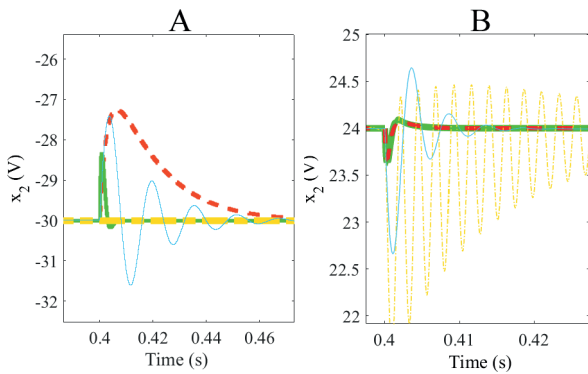


Fig. 6. Software simulation result (Matlab/Simulink) using control techniques SFL (dashed red), D-SFL (continue green) D-CICAPBC (continue cyan), D-IDAPBC (dashed yellow). Output voltage  $x_2$  for buck-boost (A) and buck (B) in view of input variation (50  $\rightarrow$  30 V) in 0.4s.

**TABLE VIII**  
Initial and Converters Parameters

Parameters	Buck-boost	Buck
$x_{1d}$	$\frac{G}{E} V_d^2$	$GV_d$
$R$	10 $\Omega$	10 $\Omega$
$L$	322 $\mu$ H	322 $\mu$ H
$C$	400 $\mu$ F	400 $\mu$ F
$E$	50 V	50 V
$V_d$	-30 V	25 V
$f$	50 kHz	50 kHz
$k_1$	3	3
$k_z$	-300	-500
$k_{int}$	-300	-300
$k_\alpha$	0,77	0,77

**TABLE IX**  
Experimental Buck

$x_{1d}$	$\frac{G}{E} V_d^2 = 1A$
$R$	4 $\Omega$
$L$	322 $\mu$ H
$C$	400 $\mu$ F
$E$	24 V
$V_d$	12 V
$f$	20 kHz
$k_1$	6
$k_{int}$	5

and the inductor current for a step variation of setpoint  $x_{1d} = 1A \Rightarrow 3 A$ . The output reference voltage  $V_d$  is set initially to 4 V, at  $t = 2$  ms it changes to 12 V and at  $t = 14$  ms returns to 4 V. Figure 9 presents the details of experimental waveforms. As it is shown in Figures 10 and 11, during the first 10 ms, both PI and D-SFL controllers regulate the output voltage at the desired level after transient.

The regulator design is typically driven by specifications concerning the required closed loop speed of response or,

equivalently, the maximum allowed tracking error with respect to the reference signal. These specifications can be turned into

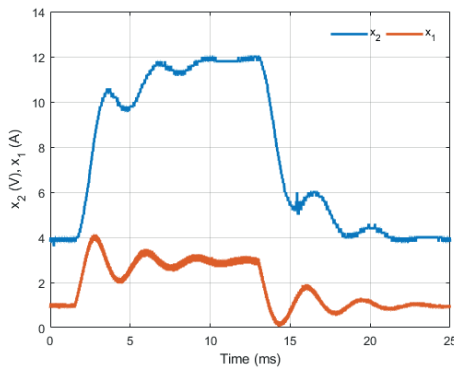


Fig. 7. Experimental result for buck - PI. Output voltage and inductor current - Setpoint variation.

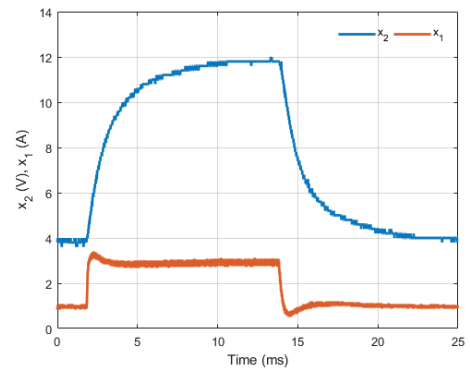


Fig. 8. Experimental result for buck - D-SFL. Output voltage and inductor current- Setpoint variation.

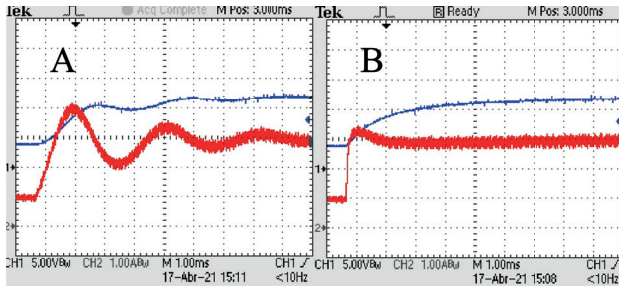


Fig. 9. Details of experimental results for buck - PI (A) and D-SFL (B). Output voltage (blue) and inductor current (red) - 12 V Setpoint.

equivalent specifications for the closed loop bandwidth and phase margin [34]. In our case, the current controller, a closed loop bandwidth equal to about 1/5 of the switching frequency ( $f_c = 20$  kHz), to be achieved with, at least, a 60 degrees phase margin.

In order to test the d-transform property of the controllers, the value of input voltage  $E$  is changed ( $24V \Rightarrow 12V \Rightarrow 24V$ ) as shown in Figures 10 and 11. It is possible to verify that the D-SFL response presents less oscillations and smaller overshoot. Thus, the phase margin is greater for D-SFL compared with the classical PI.

## VI. CONCLUSION

A new family of nonlinear controllers was proposed using the D-transform. In a new way, this method has a potentially useful properties for power converter applications. Based on the boost converter, control laws were generated for the buck and buck-boost converters (new  $d$  and new  $\delta$ ). Different alternatives were presented to show more than one way to find other candidates, which are proved to be stable control laws and eventually to present better performance.

The main contribution of this paper is to open new possibilities of stable nonlinear control laws for dc-dc converters, by a simple and direct methodology. It should be noted that the result obtained for the buck-boost – shown in Figures 5.a and 6.a (yellow line) – is quite feasible and contains the following advantages:

- low overshoot under load and input variations;
- rapid response speed;
- does not require the measurement of the inductor current

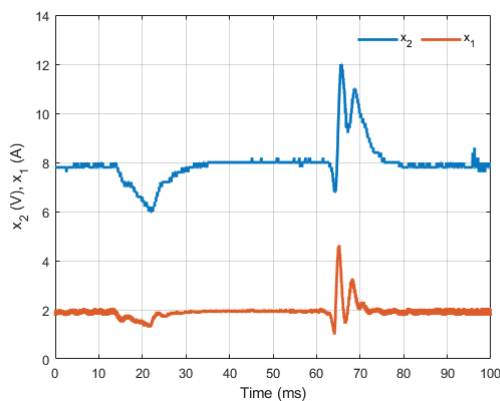


Fig. 10. Experimental result for buck - PI. Output voltage and inductor current with change of input voltage.

- $x_1$  simplifying the controller design;
- low number of counts (compared with the work of [35]).

Future research will concentrate in generalized stability proof of the transformations and the application extension to SEPIC, CUK and Three-phase converters. Additionally, the inverse process of generating equations having the buck and buck-boost as base converters will be investigated.

## ACKNOWLEDGEMENT

This work has been supported by the Brazilian agency CAPES.

## REFERENCES

- [1] G. Garcia, O. Lopez Santos, “A Unified Approach for the Control of Power Electronics Converters. Part I—Stabilization and Regulation”, *Applied Sciences*, vol. 11, no. 2, p. 631, January 2021.
- [2] S. K. Mazumder, A. Kulkarni, S. Sahoo, F. Blaabjerg, A. Mantooth, J. Balda, Y. Zhao, J. Ramos-Ruiz, P. Enjeti, P. Kumar, *et al.*, “A review of current research trends in power-electronic innovations in cyber-physical systems”, *IEEE Journal of Emerging and Selected Topics in Power Electronics*, January 2021.
- [3] Q. Xu, N. Vafamand, L. Chen, T. Dragičević, L. Xie, F. Blaabjerg, “Review on advanced control technologies for bidirectional dc/dc converters in dc microgrids”, *IEEE Journal of Emerging and Selected Topics in Power Electronics*, March 2020.
- [4] C. A. Albugeri, N. C. Dal Pont, T. K. Jappe, S. A. Mussa, T. B. Lazzarin, “Control system for multi-inverter parallel operation in uninterruptible power systems”, *Eletrônica de Potência-SOBRAEP*, vol. 24, no. 1, pp. 37–46, Março 2019.
- [5] R. G. Cacao, T. B. Lazzarin, M. C. Villanueva, I. Barbi, “Study of High Step-Up Gain DC-DC Converters Based on Stacking of Non-Isolated Topologies”, *Eletrônica de Potência-SOBRAEP*, vol. 23, no. 4, pp. 505–515, Dezembro 2018.
- [6] H. Lee, V. Smet, R. Tummala, “A review of sic power module packaging technologies: Challenges,

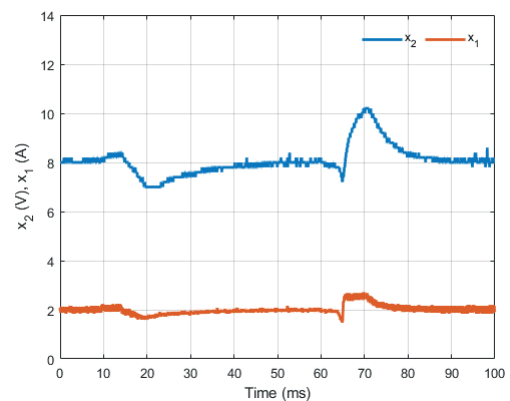


Fig. 11. Experimental result for buck - D-SFL. Output voltage and inductor current with change of input voltage.



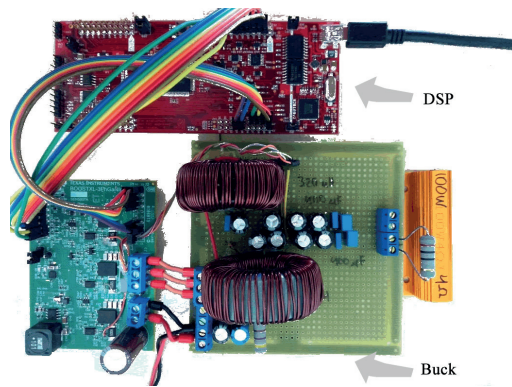


Fig. 12. DC-DC converter prototype

advances, and emerging issues”, *IEEE Journal of Emerging and Selected Topics in Power Electronics*, vol. 8, no. 1, pp. 239–255, November 2019.

- [7] J. Feng, W. Chu, Z. Zhang, Z. Zhu, “Power electronic transformer-based railway traction systems: Challenges and opportunities”, *IEEE Journal of Emerging and Selected Topics in Power Electronics*, vol. 5, no. 3, pp. 1237–1253, March 2017.
- [8] M. Elkazaz, M. Sumner, D. Thomas, “Energy management system for hybrid PV-wind-battery microgrid using convex programming, model predictive and rolling horizon predictive control with experimental validation”, *International Journal of Electrical Power & Energy Systems*, vol. 115, p. 105483, February 2020.
- [9] P. Ewald, R. V. Tambara, H. A. Gründling, “A direct discrete-time reduced order robust model reference adaptive control for grid-tied power converters with LCL filter”, *Revista Eletrônica de Potência*, vol. 25, no. 3, pp. 361–372, Setembro 2020.
- [10] M. A. Mohamed, H. M. Abdullah, M. A. El-Meligy, M. Sharaf, A. T. Soliman, A. Hajjiah, “A novel fuzzy cloud stochastic framework for energy management of renewable microgrids based on maximum deployment of electric vehicles”, *International Journal of Electrical Power & Energy Systems*, vol. 129, p. 106845, July 2021.
- [11] J. He, D. Zhang, D. Torrey, “Recent advances of power electronics applications in more electric aircrafts”, in *2018 AIAA/IEEE Electric Aircraft Technologies Symposium (EATS)*, pp. 1–8, July 2018.
- [12] B. Zhou, Y. Meng, W. Huang, H. Wang, L. Deng, S. Huang, J. Wei, “Multi-energy net load forecasting for integrated local energy systems with heterogeneous prosumers”, *International Journal of Electrical Power & Energy Systems*, vol. 126, p. 106542, March 2021.
- [13] P. T. Krein, J. A. Galtieri, “Active Management of Photovoltaic System Variability with Power Electronics”, *IEEE Journal of Emerging and Selected Topics in Power Electronics*, vol. 9, no. 6, pp. 6507–6523, July 2020.
- [14] G. V. Hollweg, P. J. Ewald, G. G. Koch, E. Mattos, R. V. Tambara, H. A. Gründling, “Controlador Robusto Adaptativo Super-Twisting Sliding Mode por Modelo de Referência para Regulação das Correntes Injetadas em Redes Fracas por Inversores Trifásicos com Filtro LCL”, *Revista Eletrônica de Potência*, vol. 26, no. 2, pp. 1–12, Junho 2021.
- [15] A. Rosa, L. Morais, G. Fortes, S. S. Júnior, “Practical considerations of nonlinear control techniques applied to static power converters: A survey and comparative study”, *International Journal of Electrical Power & Energy Systems*, vol. 127, p. 106545, May 2021.
- [16] J. F. Silva, S. F. Pinto, “Linear and nonlinear control of switching power converters”, in *Power Electronics Handbook*, pp. 1141–1220, Elsevier, 2018.
- [17] F. Vatansever, N. Yalcin, “e-Signals&Systems: A web-based educational tool for signals and systems”, *Computer Applications in Engineering Education*, vol. 25, no. 4, pp. 625–641, April 2017.
- [18] O. Gehan, E. Pigeon, T. Menard, M. Pouliquen, H. Gualous, Y. Slamani, B. Tala-Ighil, “A nonlinear state feedback for DC/DC boost converters”, *Journal of Dynamic Systems, Measurement, and Control*, vol. 139, no. 1, p. 011010, September 2017.
- [19] S. Arora, P. Balsara, D. Bhatia, “Input-Output Linearization of a Boost Converter with Mixed Load (Constant Voltage Load and Constant Power Load)”, *IEEE Transactions on Power Electronics*, vol. PP, no. 99, pp. 1–9, March 2018.
- [20] M. Zhang, R. Ortega, Z. Liu, H. Su, “A new family of interconnection and damping assignment passivity-based controllers”, *International Journal of Robust and Nonlinear Control*, vol. 27, no. 1, pp. 50–65, January 2017.
- [21] V. V. Paduvali, R. Taylor, L. R. Hunt, P. Balsara, “Mitigation of Positive Zero Effect on Nonminimum Phase Boost DC–DC Converters in CCM”, *IEEE Transactions on Industrial Electronics*, vol. 65, no. 5, pp. 4125–4134, October 2018.
- [22] Y. Zhang, J. Liu, Z. Dong, H. Wang, Y. Liu, “Dynamic performance improvement of diode–capacitor-based high step-up dc–dc converter through right-half-plane zero elimination”, *IEEE Transactions on Power Electronics*, vol. 32, no. 8, pp. 6532–6543, October 2017.
- [23] H. J. Sira-Ramirez, R. Silva-Ortigoza, *Control design techniques in power electronics devices*, Springer Science & Business Media, 2006.
- [24] R. W. Erickson, D. Maksimovic, *Fundamentals of power electronics*, Springer Science & Business Media, 2007.
- [25] H. Rodriguez, R. Ortega, G. Escobar, “A new family of energy-based non-linear controllers for switched power converters”, in *Industrial Electronics, 2001. Proceedings. ISIE 2001. IEEE International Symposium on*, vol. 2, pp. 723–727, June 2001.
- [26] H. Sira-Ramirez, R. A. Perez-Moreno, R. Ortega, M. Garcia-Esteban, “Passivity-based controllers for the stabilization of DC-to-DC power converters”, *Automatica*, vol. 33, no. 4, pp. 499–513, April 1997.
- [27] S. Sastry, *Nonlinear systems: analysis, stability, and control*, vol. 10, Springer Science & Business Media, 2013.

- [28] S. I. Seleme, L. M. F. Morais, A. H. R. R., L. A. B. Torres, “Stability in passivity-based boost converter controller for power factor correction”, *European Journal of Control*, vol. 19, no. 1, pp. 56–64, January 2013.
- [29] C. Wang, D. Sun, W. Gu, “Stability Analysis of Constant Current Controlled Primary-Side Regulation Flyback Converter”, *IEEE Journal of Emerging and Selected Topics in Power Electronics*, July 2020.
- [30] A. H. Rosa, L. M. Morais, T. M. de Souza, I. Seleme, “Comparison of nonlinear control techniques applied to SEPIC and CUK converters with reduced modeling and hybrid solutions”, in *2016 12th IEEE International Conference on Industry Applications (INDUSCON)*, pp. 1–8, 2016.
- [31] M. Zhang, P. Borja, R. Ortega, Z. Liu, H. Su, “PID Passivity-Based Control of Port-Hamiltonian Systems”, *IEEE Transactions on Automatic Control*, vol. 63, no. 4, pp. 1032–1044, April 2018.
- [32] A. Rosa, M. Silva, M. Campos, R. Santana, W. Rodrigues, L. Morais, S. Seleme Jr., “SHIL and DHIL Simulations of Nonlinear Control Methods Applied for Power Converters Using Embedded Systems”, *Electronics*, vol. 7, no. 10, p. 241, October 2018.
- [33] Texas Instruments, “BOOSTXL-3PHGANINV 48-V Three-Phase Inverter With Shunt-Based In-Line Motor Phase Current Sensing Evaluation Module”, <https://www.ti.com/tool/BOOSTXL-3PHGANINV>, online; accessed 17 April 2021.
- [34] S. Buso, P. Mattavelli, “Digital control in power electronics”, *Synthesis Lectures on Power Electronics*, vol. 5, no. 1, pp. 1–229, March 2015.
- [35] W. He, C. A. Soriano-Rangel, R. Ortega, A. Astolfi, F. Mancilla-David, S. Li, “Energy shaping control for buck–boost converters with unknown constant power load”, *Control Engineering Practice*, vol. 74, pp. 33–43, May 2018.

#### BIOGRAPHIES

**Arthur Hermano Rezende Rosa**, Bachelor’s at Control and Automation Engineering (2007), master’s at Electric Engineering (2011) and PhD at Electric Engineering from Universidade Federal de Minas Gerais (2015). Has experience in Electric Engineering, focusing on Control of Electronic Processes, Feedback, acting on the following subjects: passivity, nonlinear control, power factor correction, adaptive

control, dsp and applied control. He is professor of Federal Institute of Minas Gerais.

**Waner Wodson Aparecido Gonçalves Silva**, received the degree in electrical engineering from Faculdades Santo Agostinho in 2011, and the M.Sc. and PhD degree from the Federal University of Minas Gerais in 2013 /2018. He is currently an Assistant Professor with the Federal University of Itajuba, Campus Itabira, and lecturing classes on power electronics and embedded systems. His research interests include power electronic applications in renewable energy, energy storage, and embedded systems.

**Wei He** is with the School of Automation, Nanjing University of Information Science and Technology, China. His research interests include control of power electronics and nonlinear control.

**Fernando Andrade da Silva**, is a Control and Automation Engineer graduated from the Federal Institute of Minas Gerais. Currently working as an Engineering Analyst, working on innovation projects, development and implementation of solutions for the mineral sector. He has experience in the field of instrumentation, studies and specification of equipment/instruments for process control.

**Lenin Martins Ferreira Morais**, (Member, IEEE) received the B.Sc., M.Sc., and Ph.D. degrees in electrical engineering from the Federal University of Minas Gerais (UFMG), Belo Horizonte, Brazil, in 2000, 2002, and 2007, respectively. He completed a Postdoctoral Internship in Laboratoire Laplace, Toulouse, France. He is currently an Associate Professor with the Federal University of Minas Gerais, Belo Horizonte, Brazil, has experience in electrical engineering, with emphasis in industrial electronics, systems and electronic controls, working mainly in the subjects, including power electronics, high efficiency converters, LEDs drivers, PFC converters, PWM techniques, and solid-state transformer.

**Seleme Isaac Seleme Jr**, received the B.S. degree in electrical engineering from the Escola Politecnica (USP), São Paulo, Brazil, in 1977, the M.S. degree in electrical engineering from the Federal University of Santa Catarina, Florianópolis, Brazil, in 1985, and the Ph.D. degree in control and automation from the Institut National Polytechnique de Grenoble, France, in 1994. He is currently a Full Professor with the Department of Electronic Engineering, Federal University of Minas Gerais, Belo Horizonte, Brazil. His main research interests include renewable energy systems, modular multilevel converters, and nonlinear control applied to power converters.